



ارائه شده توسط:

سایت ترجمه فا

مرجع جدیدترین مقالات ترجمه شده

از نشریات معتبر



Comparative study on a jacket launching operation in South China Sea



Zhihuan Hu, Xin Li*, Jun Li, J.M. Yang

State Key Laboratory of Ocean Engineering, Shanghai Jiao Tong University, Shanghai 200240, China

ARTICLE INFO

Article history:

Received 12 May 2015

Accepted 18 November 2015

Available online 1 December 2015

Keywords:

Jacket launching operation

Field measurement

Model test

Numerical simulation

Comparative study

ABSTRACT

Launching is an essential initial operation for mega deep-water jackets. The forces and motion responses of key points were measured during such a launching operation, which can serve as a benchmark for the experimental and numerical results and hence can provide more confidence in following operations. This paper presents a comprehensive study in which field measurements, numerical and experimental results are compared to investigate the dynamic process of launching a mega jacket. The differences between the field measurement data and experimental results are investigated. The sensitivity analyses including the barge trim and draft and the friction coefficient along the skid-ways are performed using the calibrated numerical model. Attempts are made to clarify the effect of the drag coefficient in the Froude-similarity models through a comparison of the scaled model tests and the specific numerical simulations.

© 2015 Elsevier Ltd. All rights reserved.

1. Introduction

Launching is one of the critical tasks during offshore installation of a jacket and involves considerable risks and technical challenges, particularly for mega jackets. As the jacket slides along the skid-ways, the draft and trim of the launching barge keep changing, thereby affecting the motion response of the barge. Once the jacket begins to tip on the rocker arms, which is the most hazardous stage of the operation, the rocker arm loads reach their peak values. After separating from the barge, the jacket oscillates and dives to reach its maximum dive depth, where it could collide with the seabed. Therefore, it is important to reliably predict the forces and motion responses of such a launching system.

To correctly predict the key motion responses, numerous studies of jacket launching operation have been conducted. Hambro (1982) proposed a method to compute the jacket motions by differentiating the constraints of the mechanical systems twice. A model test was selected to determine the accuracy of the numerical simulations. Liu et al. (1986) established three-dimensional equations of motion for a jacket by combining quadratic differentiation of the restraints with momentum equations. Good agreement was achieved between the numerical and experimental results. Based on the Kilauea jacket launching, Sircar et al. (1990) described the method and results of the transportation, launching, self-upending and set-down stability analyses. Honarvar et al. (2008) compared a model test and a numerical simulation of jacket launching operation. The differences between

the experimental and numerical results were identified, and the correlation between the Reynolds number (Re) and the hydrodynamic drag coefficient (C_D) was discussed.

When considering the structural loads and the motion responses, model tests and numerical simulations were also performed for the launching operation. Jo et al. (2001) presented the effects of various parameters (the dimensions of the barge and jacket and the initial condition of the barge) on the launching operation based on the analysis software SACS. The results showed that the mean load and impact load acting on the jacket could be reduced by increasing the draft and trim angle, whereas the trim angle and draft had a marginal effect on the dive depth of the jacket. Xiong et al. (2013) investigated a typical jacket launching process by comparing model tests and numerical simulations. These authors reported good agreement between the amplitudes of the pitch motion and structural load using two different methods. A time delay was also observed in the model test due to the scale effect. He et al. (2010) presented an optimization study and a parametric sensitivity study of 3-D time-domain launching and self-upending analyses through the commercial software MOSES. In the optimization study, the optimal initial conditions were determined for the jacket launching and upending.

To obtain a better understanding of jacket launching, efforts have been made to develop reliable techniques for field measurements. Based on the field measurements of the Liwan 3-1 mega jacket launching, a series of the jacket launching analyses was conducted. He et al. (2013) performed a comparative study based on numerical analyses and field measurements, which indicated that the effect of the kinetic friction coefficient (C_f) along the skid-ways was significant. Zhang et al. (2013) conducted an experiment to investigate the launching trajectories and further

* Corresponding author.

E-mail address: lixin@sjtu.edu.cn (X. Li).

compared the experimental results with field measurements. This study indicated that C_f along the skid-ways should be reduced to 0.04 to ensure kinematic similarity. A method of processing the original data from the field measurement was proposed by Chen et al. (2013). In their study, the composite Simpson's rule was applied to obtain the trajectory motions of the jacket and barge. These trajectory motions were obtained from the field measurement of the Liwan 3-1 jacket launching and were presented by Chen et al. (2014b).

Field measurements of offshore structures and their dynamic responses in real sea states are desirable for validating numerical simulations and for applying to marine engineering design problems (Drazen et al., 2012). However, due to various technical and economic challenges, more emphasis has been placed on the in-operation platform monitoring than on the field measurements of offshore installation procedures, such as jacket launching.

This paper presents a comparative study of field measurements, scaled model tests and numerical simulations based on the field measurements obtained from the launching of the Panyu 34-1 mega jacket. Section 2 briefly describes the jacket launching system in terms of the launching stages, the launching barge and the jacket and the initial launching condition. The experimental setups are briefly presented in Section 3. The environmental conditions during the launching operation are also clarified in this section. To validate the experimental results and to further understand the dynamics of the launching, the field measurements were performed and time series of the barge and jacket motions and the rocker arm loads were measured as part of the field measurements. Section 4 discusses the configuration of the field measurement system. It is extremely important to ensure that the measurements obtained during the jacket launching operation are sufficiently reliable and valid and thus the measurement equipment and measurement errors are also given in Section 4. Based on the field measurement data, the numerical simulations are validated and calibrated. Section 5 briefly gives the theoretical background of the jacket launching under the assumption of the stationary sea state and two-dimensional motion. By means of the calibrated numerical model, sensitivity analyses are performed to clarify the influences of the barge trim angle and draft, the jacket center of gravity (COG) and the kinetic friction coefficient along the skid-ways. The drag coefficients in the scaled models and prototype are discussed and the effects of C_D in the Froude-similarity models are also investigated in Section 6. Conclusions are presented based on the results and discussions to guide safe launching operations, and for the future offshore installations.

2. Jacket launching system

The jacket was successfully launched and installed in 190 m-deep waters with the assistance of the launching barge. To describe the motion of the jacket launching system, two coordinate systems are introduced: the global coordinate system ($O_g - x_g y_g z_g$) and body-fixed coordinate system. As shown in Fig. 1, the former system is fixed with respect to the earth, and its x - y -plane coincides with the water surface. The jacket-fixed coordinate system ($O_j - x_j y_j z_j$) moves with the jacket and its x - y -plane coincides with the jacket waterline. In addition, the barge-fixed coordinate system ($O_b - x_b y_b z_b$) moves with the barge and its x - y -plane coincides with the barge keel. The origin of each coordinate system is located in the central plane for simplicity.

2.1. Launching barge and jacket

The T-shaped launching barge features its narrower bow half and wider stern half, which contributes to a larger displacement and a better transverse stability (Xu et al., 2013). Its trim angle can be adjusted using the ballast tanks to initiate launching and to ensure the stability of the entire launching system. The transverse metacentric height of the barge is 11.6 m in the initial launching condition (draft=11.12 m, trim=4.25°). The barge is equipped with skid-ways, two identical rocker arms and installation aids and ancillary equipment. Tilting beams and a pair of rocker arms are attached in the stern of the barge. The length of each rocker arm is 41.14 m and the depth of the tilt beam is 7.54 m. The principal parameters of the barge are described in Table 1.

The eight-legged jacket is 203.5 m tall and is secured to the seafloor with $16 \times \varnothing 108'' (2743 \text{ mm}) \times 143.3 \text{ m}$ foundation piles. Its reserve buoyancy is approximately 12.31% under the condition of void members. The principal parameters of the jacket are described in Table 2.

2.2. Launching condition

To initiate the launching, the barge was ballasted to the launching condition with the mid-ship draft of 11.12 m and trim of 4.25°. Fig. 2 shows the top view of the initial launching system. As shown in Fig. 2, the horizontal distance between the jacket COG and the mid-ship section is approximately 16.6 m.

There is a pair of steel skid-ways on the barge deck. The horizontal interval between the two skid-ways is 24 m and the overall length of each one is 150 m. Fig. 3 shows a cross section of the skid-way. As shown in Fig. 3, a pair of steel cradle is welded onto the jacket member and slides along with the jacket. The grease and Teflon coating are applied to the contact surface of the skid-ways and the launch cradles. The kinetic friction coefficient are in

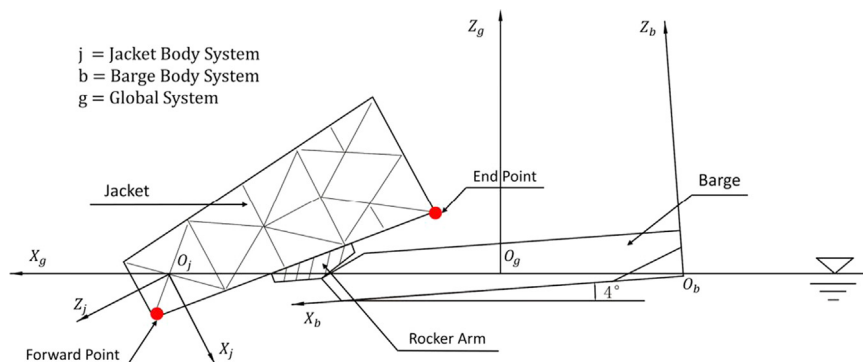


Fig. 1. Launching system configuration.

the range of 0.03–0.08 for the wood-grease-Teflon contact surface (Denton, 2013).

2.3. Launching stages

The launching operation can be divided into four stages:

- (1) Ballasting stage: the barge is ballasted to achieve the desired trim and draft.
- (2) Sliding stage: the jacket slides on the barge due to its self-weight without tipping of the rocker arms.

Table 1

Principal parameters of the launching barge. The displacement and metacentric heights are those of the initial launching condition (trim=4.25°, draft=11.12 m).

Items	Symbol	Unit	Value
Length between perpendiculars	L_{pp}	m	215.0
Fore-body breadth moulded	B_{Fore}	m	42
Aft-body breadth moulded	B_{Aft}	m	65
Depth moulded	D	m	14.25
Longitudinal centre of gravity from FP	LCG	m	116.3
Transverse centre of gravity from CL	TCG	m	0.00
Vertical centre of gravity above BL	VCG	m	8.15
Displacement	Δ	MT	125,293
Transverse metacentric height	GM_T	m	11.6
Longitudinal metacentric height	GM_L	m	98.1

Table 2

Principal parameters of the PY34-1 mega jacket. The metacentric heights are those of the free floating condition.

Items	Symbol	Unit	Value
Height	H	m	203.5
Length at top	L_t	m	50
Length at bottom	L_b	m	82
Breadth at top	B_t	m	34
Breadth at bottom	B_b	m	82
Weight	W	MT	23,312
Buoyancy when fully submerged	B	MT	27,279
X coordinate of the centre of gravity	X_{CG}	m	-0.03
Y coordinate of the centre of gravity	Y_{CG}	m	-1.27
Z coordinate of the centre of gravity	Z_{CG}	m	-115.3
Radius of roll gyration	R_{xx}	m	67.41
Radius of pitch gyration	R_{yy}	m	66.52
Radius of yaw gyration	R_{zz}	m	39.04
Intact transverse metacentric height	GM_T	m	1.0
Intact longitudinal metacentric height	GM_L	m	0.97

- (3) Tipping stage: the jacket slides with tipping of the rocker arms until the rocker arms rotate up to the maximum allowable angle and the jacket is launched into the sea.
- (4) Self-righting stage: The jacket, once freed from the barge, oscillates a few times and comes to rest.

In this paper, the sliding stage and tipping stage are investigated in detail, because these two phases are of most concern.

3. Experimental setups

Model tests of jacket launching are performed to confirm that no important facet of the operation has been overlooked before the field launching. In the model tests, Froude's scaling law was used based on the effects of gravitational acceleration and such tests were performed using a scale of 1:50 in the wave basin of State Key Laboratory of Ocean Engineering. For the field launching operation, it usually lasts less than 80 s from the sliding stage to self-righting stage. It is common to assume that the sea surface is stationary for a duration of 20 min to 3–6 h (DNV, 2014). Thus the model test with the base condition (draft=11.12 m, trim=4.25°) was recreated in a stationary sea state.

3.1. Experimental instruments

The launching models consisted of a steel jacket, a barge, sliding equipment, rocker arms and several experimental instruments. And the model of the sliding equipment consisted mainly of launch cradles and a pair of skid-ways, which were attached to the jacket member and the barge deck, respectively. Fig. 4 shows a cross section of the sliding equipment. As shown in Fig. 4, lubricating oil and Teflon coatings were used to reduce the friction coefficient.

Two noncontact optical systems consisting of camera and markers were used to measure the motion responses of the launching system (Zhao et al., 2014). Such cameras can receive the light reflected by each marker and then capture the motion of each body with the measurement error of 0.1 mm. In addition, four one-dimensional pressure sensors were installed under the rocker arms to measure the rocker arm loads, as shown in Fig. 5. The measuring range and measurement error of such sensors are 50 kg and 0.5 kg, respectively. To initiate the launching, electromagnet is used for the release of the jacket. When the current is turned off, the magnetic field disappears and the jacket begins to slide on the barge.

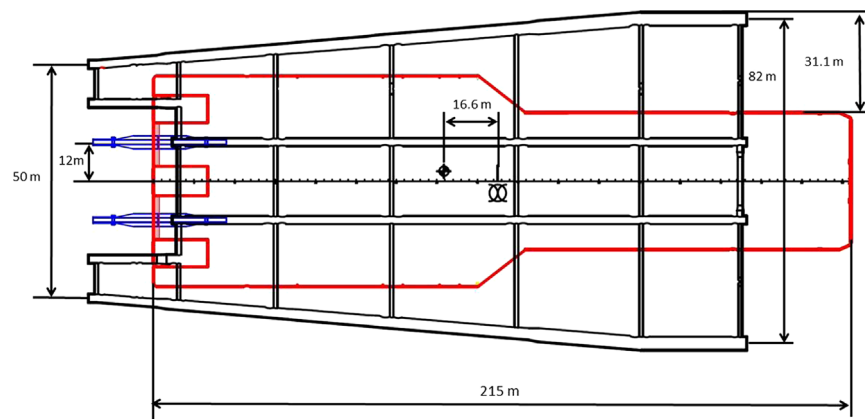


Fig. 2. Top view of jacket launching system in the initial condition.

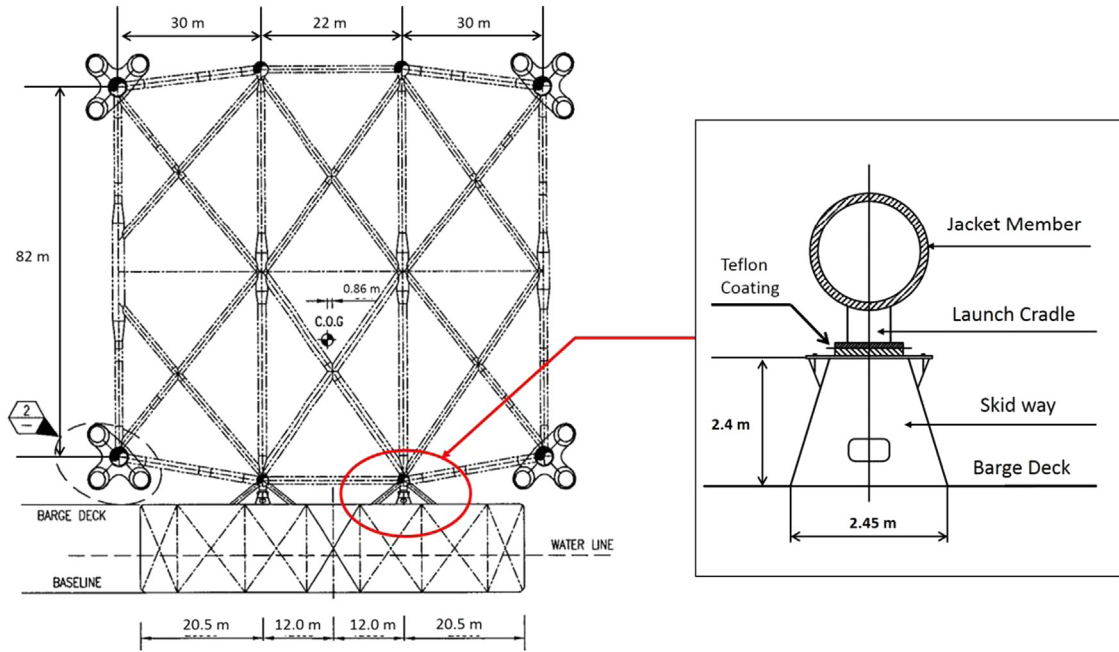


Fig. 3. Details of skid-ways.

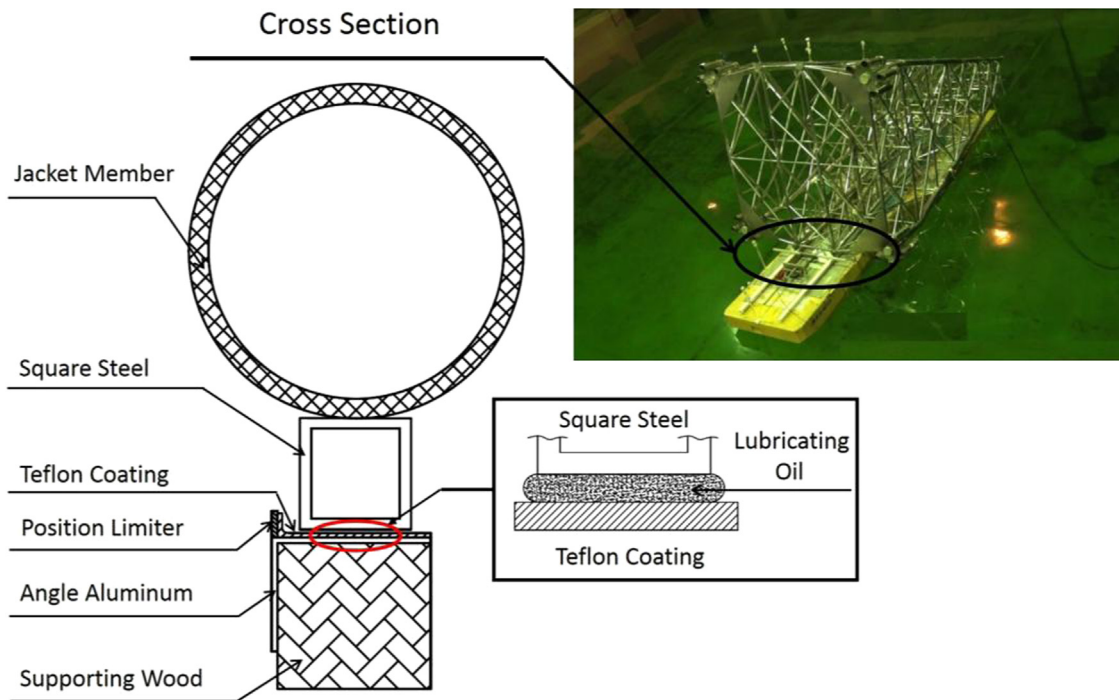


Fig. 4. Cross section of sliding equipment.

3.2. Calibration of launching system

In all stages, the dimensions and mass characteristics (mass, COG and inertia) of the jacket, barge and rocker arms were carefully measured and calibrated in accordance with the design values. Specifically, lead bars were adopted and the locations of these lead bars were adjusted inside the jacket members. The inertial properties of barge were also verified by weighting the barge model.

The friction coefficient along the skid-ways is also one of the main parameters for the launching operation. In the model test, an

Atwood machine with dragging a block over a horizontal surface (Eagleson, 1945). As shown in Fig. 6, the block of mass m_1 is initially accelerated when connected to a driving weight of mass m_2 . Once the driving weight reaches a specified distance h , the moving block slows to a stop. Then, the kinetic friction coefficient can be given by:

$$C_f = \frac{m_2 h}{m_1 h + (m_1 + m_2) d} \tag{1}$$

Based on the tests for determining the coefficients of sliding friction, C_f along the skid-ways was 0.06.

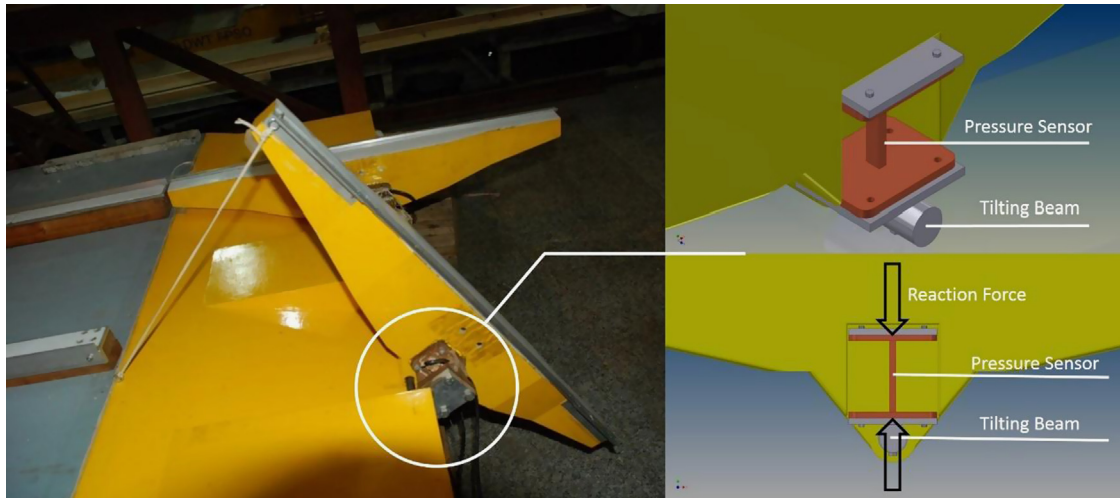


Fig. 5. Schematic of pressure sensors.

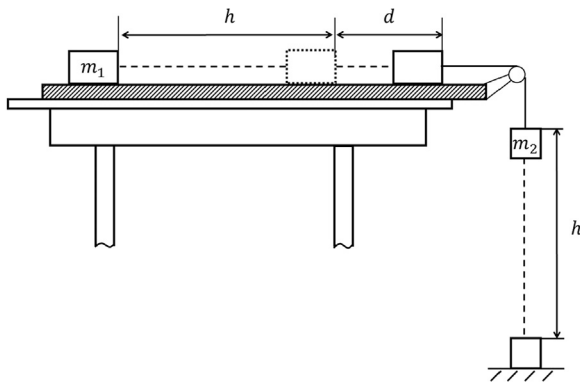


Fig. 6. Sliding friction coefficient measurement setup.

4. Field measurement system configuration

4.1. Integrated GPS and INS system

An inertial navigation system (INS) can be integrated with a global positioning system (GPS) to estimate the generalized position and velocity in 6 degrees of freedom (DOFs) (Fossen, 2011). More specifically, the GPS is capable of accurately recording the positions from two GPS antennas without drift error. However, GPS functions only above the water surface because the satellite signals are poor underwater. Meanwhile, the INS, which is housed inside a watertight barrel, can effectively record underwater motions. For the integrated GPS and INS system, the position errors are 2.0 m in horizontal direction and 4.0 m in vertical direction, respectively. And its attitude error is 0.1° . The steel alloy barrel is capable of withstanding water pressures of 3.0 MPa and features mechanical seal equipment and watertight connectors that prevent water from entering the barrel through screw threads or coaxial cables. Additionally, when fully charged, the Li-ion battery in the barrel can power the GPS/INS device for 24 h. Details of the integrated GPS/INS device are shown in Fig. 7.

In the field, two sets of the integrated GPS/INS devices were welded onto the jacket and one was installed on the barge. Fig. 7 shows the installation locations of the jacket-mounted GPS/INS systems. The locations of the GPS antennas were purposely selected to ensure adequate timing to receive GPS signals and ensure the shortest distance to the integrated GPS/INS device. The

signal amplifier was designed to address the problem of signal attenuation. And the signal shielding was relatively weak due to the angle (θ) between the GPS antennas and the jacket member. For ease of access to the integrated GPS/INS device after launching, the jacket-mounted systems were installed approximately 39 m below the top of the jacket. After launching, the jacket was lifted by the crane until it reached the upright position. Fig. 8 illustrates the upending stage and the upright position of the jacket. As shown in Fig. 8, the depths of the integrated GPS/INS devices ranged from 2 to 4 m, which facilitated the removal of the integrated GPS/INS devices from the jacket.

4.2. Stress measurement

Fibre Bragg grating (FBG) strain sensors provide detailed strain information with minimal intrusion on the host structure (Tyler et al., 2013). Fig. 9 shows the installation positions of the strain gauges on each rocker arm. To minimize the random error due to temperature variations, temperature-compensating sensors were installed with the strain gauges. Specifically, the A1 and B1 sensors were used to offset the influences of water temperature and the A5 and B5 sensors provided compensation for air temperature. The sensor surfaces were covered with waterproof silica gel. The residual errors for offset corrections are typically on the order of 1–2 pm (Micron Optics, 2012).

5. Theoretical background of jacket launching operation

Under the assumption of two-dimensional motion in the vertical plane, the equation of motion in the time domain can be written as

$$\mathbf{I}\ddot{\mathbf{q}} + \mathbf{C}\dot{\mathbf{q}} + \mathbf{K}\mathbf{q} = \mathbf{s} \quad (2)$$

where, \mathbf{q} is a vector of 3 degrees of freedom. This implies that the dynamics associated with the motion in roll, yaw and sway are neglected. \mathbf{I} is the 3×3 mass matrix; \mathbf{C} and \mathbf{K} are the damping and stiffness matrices, respectively. The vector \mathbf{s} is called the excitation force.

In the case where incident waves are absent, the excitation force on the barge can be written as

$$\mathbf{s} = -\mathbf{A}\ddot{\mathbf{q}} - \int_0^t \mathbf{D}(t-\tau)\dot{\mathbf{q}}(\tau)d\tau \quad (3)$$

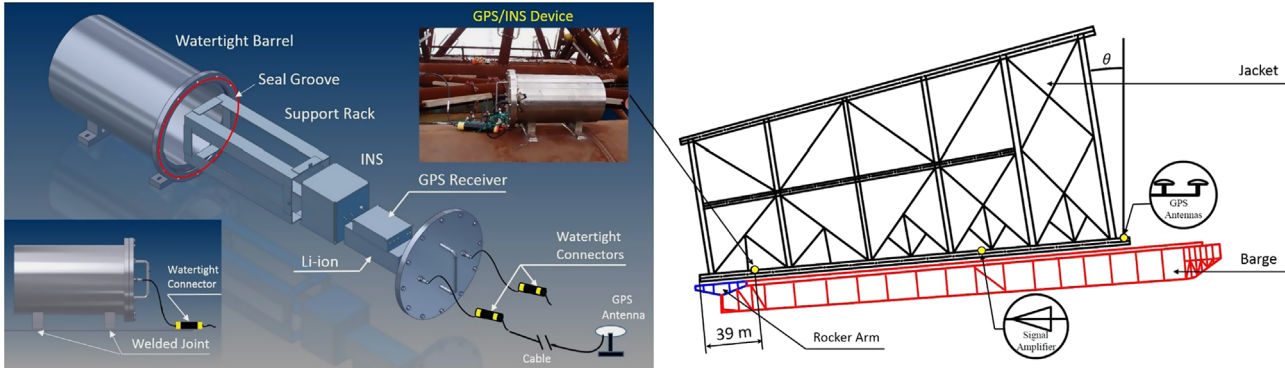


Fig. 7. GPS/INS system device.

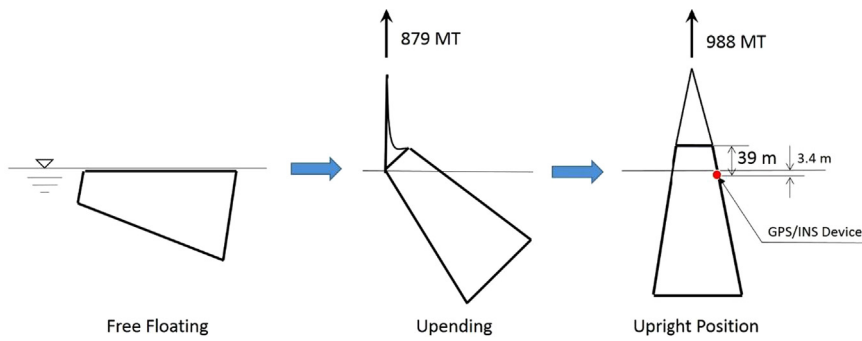


Fig. 8. Upending stage.

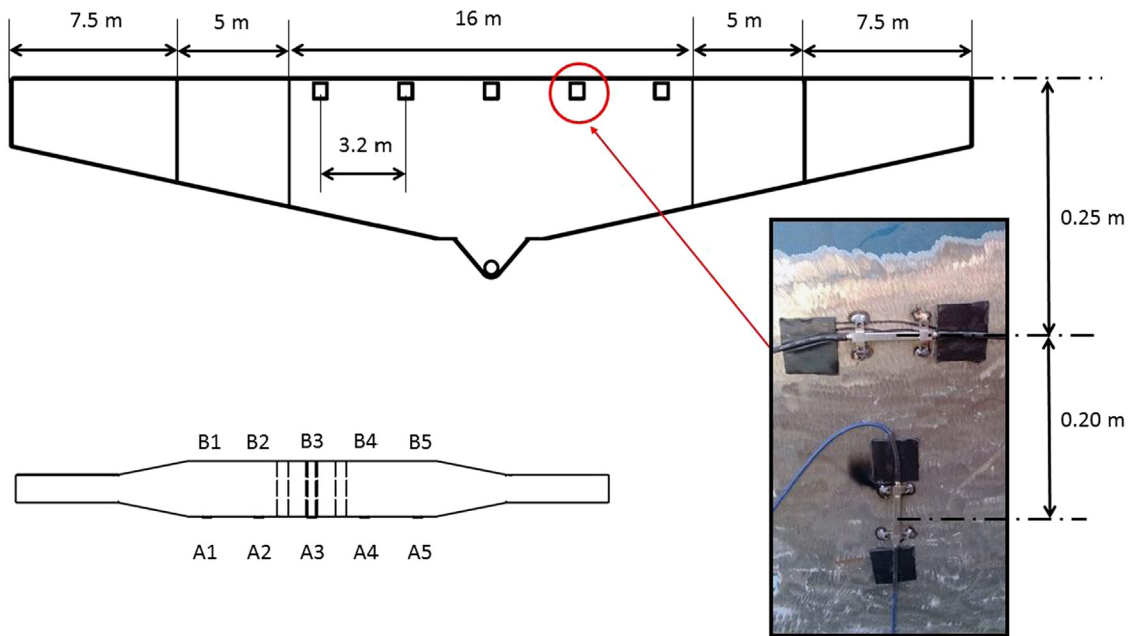


Fig. 9. Installation position of strain gauge.

where, \mathbf{A} is the added mass matrix; The kernel of the convolution term $\mathbf{D}(t)$, linked to memory effects, is the matrix of retardation functions (Chen et al., 2014a).

Jo et al. (2002) described the loads applied to such a jacket, one of which is the friction in the tangential direction.

$$\mathbf{F}_f = C_f \mathbf{F}_N \quad (4)$$

where, C_f is the friction coefficient and \mathbf{F}_N is the normal reaction force.

The hydrodynamic force on the jacket consists of drag, added mass and the hydrodynamic interactions between the two bodies. The hydrodynamic interactions are neglected in the launching analysis. The hydrodynamic force can be calculated using the equation

$$\mathbf{F}_h = C_M \rho V \dot{\mathbf{U}} - \frac{1}{2} C_D \rho A |\mathbf{U}| \mathbf{U} \quad (5)$$

where, ρ is the fluid density; V and A are the submerged volume and area, respectively; \mathbf{U} is the relative velocity between the jacket

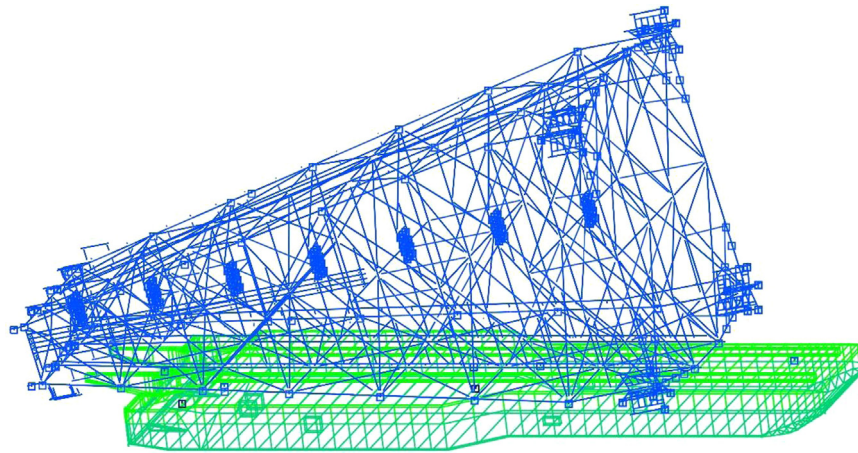


Fig. 10. Jacket launching model.

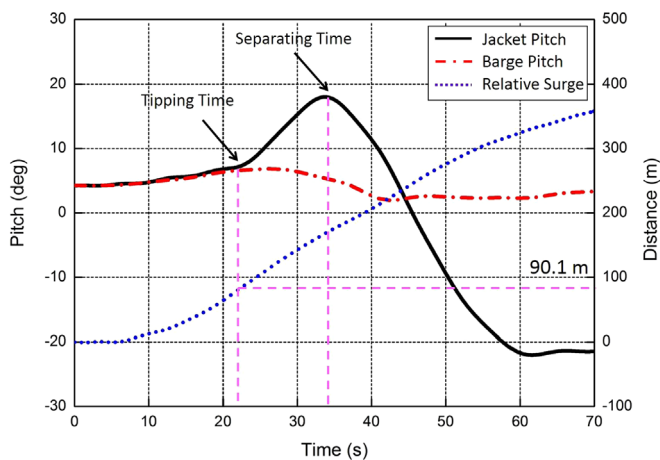


Fig. 11. Time series of the field measured longitudinal motions.

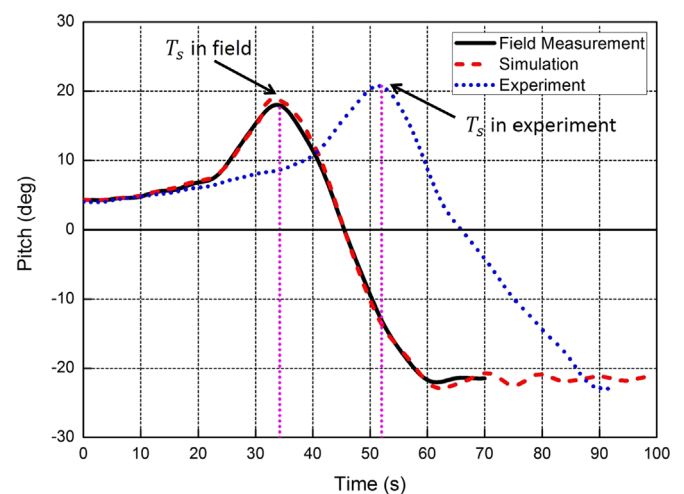


Fig. 12. Comparison of the jacket pitch motions.

member and the outer flow; C_D and C_M are called the drag coefficient and added mass coefficient, respectively.

Time domain analysis is performed using the computer software MOSES. The Newmark method is employed to provide an effective solution for the motion equations (Nachlinger, 2006). Dynamic and sensitivity analyses are also performed when considering the jacket and barge trajectory motions and the rocker arm loads. A simulation case with the parameters ($C_f=0.037$, $C_D=1.20$, $\text{Trim}=4.25^\circ$ and $\text{draft}=11.12\text{ m}$) is chosen for the numerical analysis. Fig. 10 presents the MOSES models used for the numerical simulation.

6. Results and discussions

In this section, the statistical analyses of the field data are presented. Based on the field data, the numerical methods are calibrated and validated. Efforts are made to clarify the influences of the initial condition and friction coefficient on the launching responses. Moreover, an investigation of the effect of the drag coefficient is presented.

6.1. Trajectory motions

The time series of pitch motions obtained from the numerical simulation and the experiment are compared with those from the field measurements. Furthermore, the trajectory motions of the

jacket forward point (FP) and endpoint (EP) and the transverse motion response of the launching system are investigated.

6.1.1. Pitch motions

For a successful launching operation, the pitch motions should be investigated to ensure the stability of the jacket and barge. Fig. 11 shows the time series of pitch motions and the relative sliding distance between the two bodies recorded in the field measurements. The tipping time, when the relative angle between the jacket and barge begins to increase significantly, occurs at 23.2 s. Meanwhile, the relative distance between the two bodies reaches 90.1 m (the initial distance between the jacket COG and tilting beam is 88.1 m), indicating that the jacket COG just passes over the tilting beam. The separating time, when the jacket pitch angle reaches its peak, occurs at 34.4 s. The maximum values of the pitch motion for the jacket and barge are 18.2° and 6.8° , respectively. The pitch angle of the barge stays within the design range (8.0°), which indicates the stability of the barge during launching.

The time series of the jacket pitch motion obtained from the numerical simulation, the experiment and field measurements are compared in Fig. 12. It can be seen from Fig. 12 that the numerical results agree well with the field results. The experimental results also exhibit good qualitative agreement with the field measurements. However, the launching operation in the experiment is much longer in duration than the field launching operation.

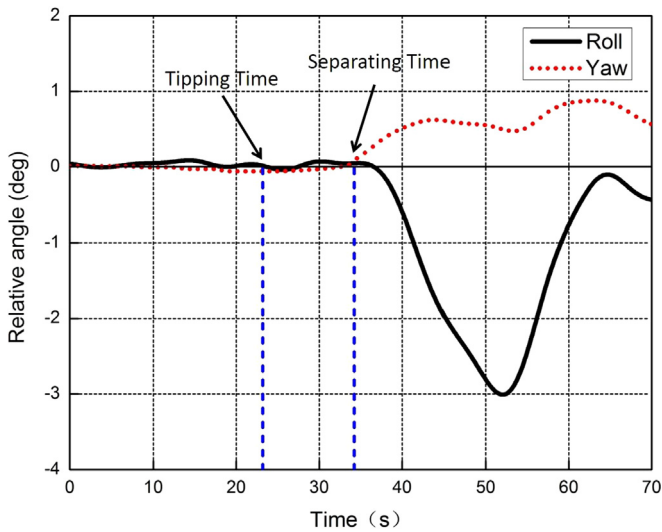


Fig. 13. Time series of relative roll and yaw motions.

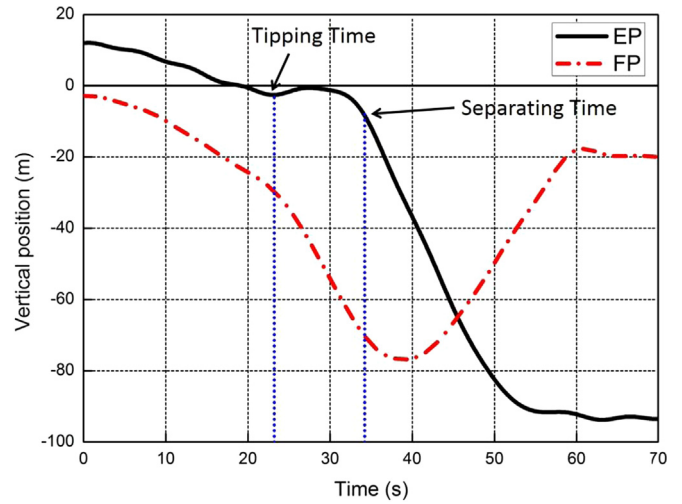


Fig. 14. Time series of jacket vertical positions in field measurement (FP and EP indicate endpoint and forward point).

Moreover, the maximum pitch angle in the experiment (20.6°) is slightly larger than that in the field measurements. It is reported that C_f along the skid-ways can introduce such discrepancies in the tipping time and separating time (He et al., 2013; Zhang et al., 2013).

6.1.2. Relative roll and yaw motions

To investigate the transverse motion responses in the field measurements, the time series of the relative roll and yaw motions between the jacket and barge are plotted in Fig. 13. As shown in Fig. 13, the relative roll angle varies between -3.0° and 0.2° , and the relative yaw angle varies within 1.0° . This demonstrates good stability of the launching operation in the transverse direction. When sliding on the skid-ways, the jacket is constrained to the barge. Therefore, the relative roll angle between the two bodies is close to 0° . Once the jacket separates from the rocker arms, minor roll and yaw angles tend to be generated due to the asymmetry of the jacket structure, such as the deviation of the transverse centre of gravity or the environmental conditions. Considering the small amplitudes of roll and yaw motions, the launching motion can be simplified to two-dimensional motion in the vertical plane. It should be noted that many undesirable events, including the structural failure or overturning of the barge, could occur if considerable relative roll and yaw motions occur between the two bodies. As the jacket weight and dimensions increase, the jacket and barge specifications should be checked to ensure the safety of the launching operation.

6.1.3. Dive depth

It is important to ensure sufficient separation between the jacket and the seabed to avoid any damage to the structure. The vertical positions of the jacket FP and EP are examined by plotting the trajectories of the two points in Fig. 14. As shown in Fig. 14, the maximum dive depths of these two points are 76.8 m and 93.8 m, respectively. This demonstrates the safe bottom clearance in the 195 m-deep waters. The vertical position of the jacket EP begins to dramatically increase at approximately 34.2 s, when the jacket separated from the barge. It oscillates and finally stabilizes at a water depth of 93.3 m. Accordingly, the maximum depth of the FP (87.2 m) is 41.4 s, and it later reaches its equilibrium position (18.7 m).

The trajectory motions obtained from the three methods are further compared in Fig. 15. For the EP, the trajectory motion in the numerical simulation strongly agrees with that in the field

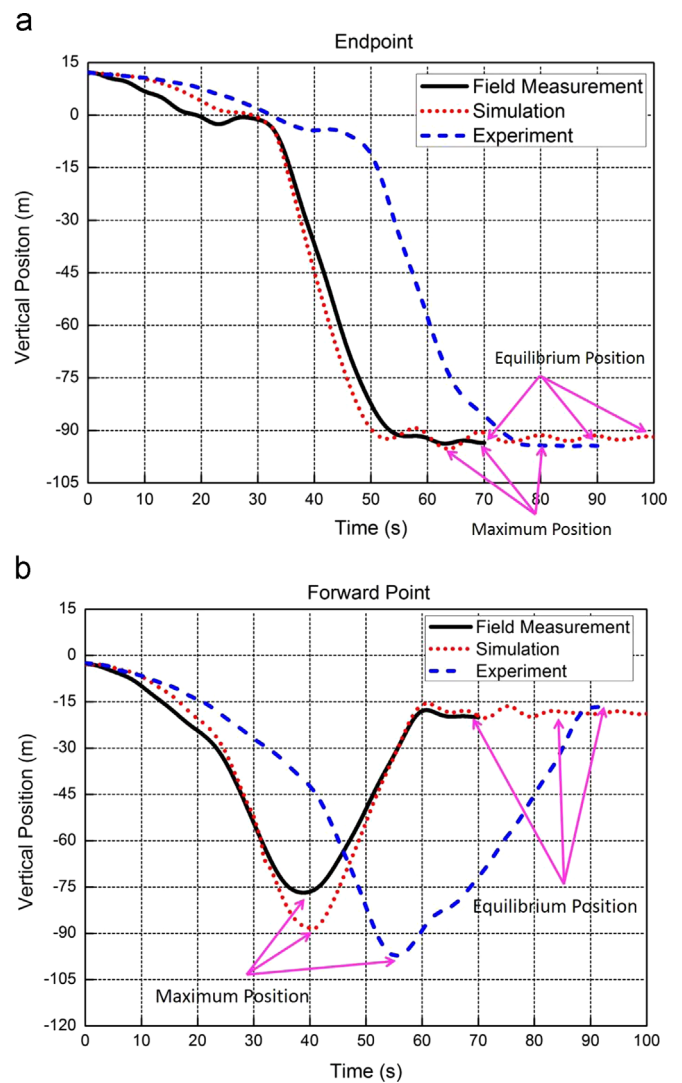


Fig. 15. Time series of FP and EP recorded by three methods.

measurements, whereas there is a time offset of approximately 15 s in the experiment. For the FP, similar motions in the vertical direction can be observed in Fig. 15(b). To more clearly describe

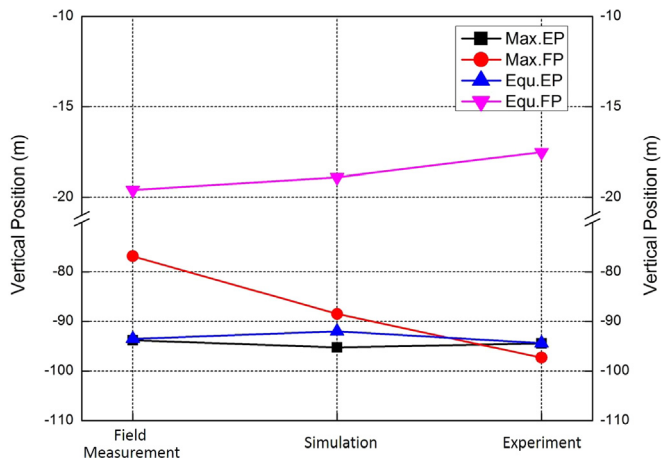


Fig. 16. Comparisons of vertical positions of FP and EP.

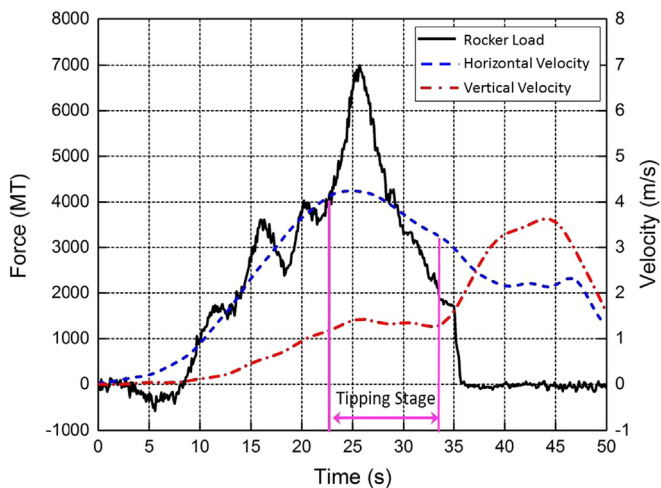


Fig. 17. Time series of jacket velocity and rocker load.

the jacket motion in the vertical direction, the maximum and equilibrium values of the jacket FP and EP are presented in Fig. 16. The dive depths of these two points at equilibrium, which can be determined from the centre of buoyancy and the centre of gravity of the jacket, are essentially consistent. However, the maximum dive depths of the FP in the numerical simulation (88.5 m) and in the experiment (97.3 m) are larger than that in the field measurement (76.1 m). Generally, the discrepancy among the three tools is more evident at the FP. Clearly, the distance between the jacket COG and the FP is much larger than that between the COG and EP. This indicates that the vertical motion of the FP is related to not only the vertical motion of jacket COG but also the jacket pitch when the jacket separates from the barge. As discussed earlier, when the jacket separates from the rocker arms, its pitch angle in the experiment (20.6°) is slightly larger than that in the numerical simulation (18.8°) and field measurement (18.2°). The larger the jacket tips, the greater depth the FP tends to reach. Moreover, there might be some influence from the field waves which have been ignored in the model tests and numerical simulations. The wave-induced motions of the barge may affect the initial launching condition, thereby affecting the jacket pitch motion and the vertical motion of the FP.

6.2. Rocker arm loads

The recorded time series of the rocker loads and the jacket velocities are presented in Fig. 17. As shown in Fig. 17, the

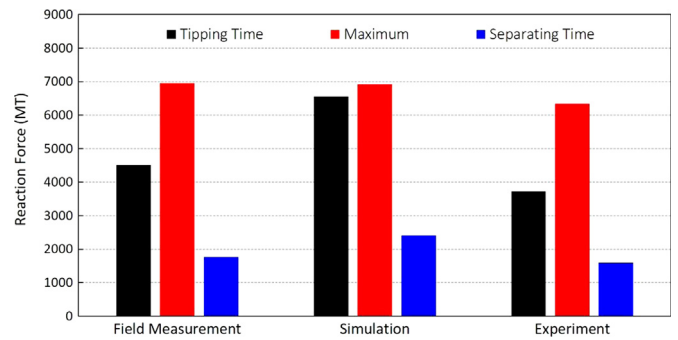


Fig. 18. Comparisons of rocker loads (tipping time and separating time indicate the rocker loads at the tipping time and separating time, respectively).

maximum rocker load (6956 MT) occurs at 25.6 s. Meanwhile, the jacket slides rapidly at a speed of 4.46 m/s. The reaction forces change rapidly during the tipping stage because the buoyancy, friction and hydrodynamic force constantly change as the jacket simultaneously rotates on and slides down the rocker arms.

To further understand the rocker arm loads, a comparisons of the three sets of results are presented in Fig. 18. Generally, good agreement is observed among the maximum values obtained from the three tools. The maximum reaction force in the numerical simulation is 0.5% larger than that recorded in the field measurement. By contrast, the maximum reaction force in the experiment is smaller than that observed in the field measurement. As discussed before, the rocker loads are decided by many factors including the sea state and the motion of the two bodies. In the following discussion, the numerical sensitivity analyses considering the effect of the initial launching conditions and drag coefficient on the maximum rocker load will be presented. In general, the maximum reaction force acting on each rocker arm is estimated to account for 29% of the jacket weight.

6.3. Sensitivity study

The initial conditions include the barge trim and draft, the longitudinal position of the jacket COG (LCG) and the kinetic friction coefficient along the skid-ways. To quantify the effects of these parameters, the critical launching responses, including the jacket pitch motion, the dive depth and the maximum rocker load under the specified conditions, are investigated. The non-dimensional values describing every type of launching response under various conditions depend on the ratio of every value to its maximum value. The sensitivity analyses are conducted using the numerical method and the relevant initial conditions are listed in Table 3.

6.3.1. Barge trim and draft

Variations of the critical launching responses against the barge trims are presented in Fig. 19. Through a comparison of these five trim conditions, one can conclude that the initial trim has a slight effect on the maximum rocker load. Taking the maximum rocker load under the trim of 3.25° as the reference, the corresponding values in case 1-2, 1-3, 1-4 and 1-5 are reduced by 1.65%, 4.80%, 8.04% and 12.9%, respectively. Clearly, a large trim leads to a reduction in the maximum rocker load. Similar trends are evident in the tipping time and separating time: a larger trim corresponds with more rapid launching. By contrast, the trim exerts no noticeable effect on the maximum dive depth. A possible contribution to this interesting phenomenon may be the jacket gravity. As the initial trim angle increases, the friction on the jacket decreases, which results in a higher sliding velocity. Moreover, the effect of increasing displacement and velocity during the tipping

Table 3
Parameters of the initial conditions.

Items	Cases	Trim (deg)	Draft (m)	LCG deviation (m)	C_f	C_d	C_m
Base condition	Case 0	4.25	11.12	0.0	0.037	1.20	1.0
Initial trim condition	Case 1-1	3.25	11.12	0.0	0.037	1.20	1.0
	Case 1-2	3.75	11.12	0.0	0.037	1.20	1.0
	Case 1-3	4.25	11.12	0.0	0.037	1.20	1.0
	Case 1-4	4.75	11.12	0.0	0.037	1.20	1.0
	Case 1-5	5.25	11.12	0.0	0.037	1.20	1.0
Initial draft condition	Case 2-1	4.25	9.50	0.0	0.037	1.20	1.0
	Case 2-2	4.25	10.00	0.0	0.037	1.20	1.0
	Case 2-3	4.25	10.50	0.0	0.037	1.20	1.0
	Case 2-4	4.25	11.12	0.0	0.037	1.20	1.0
	Case 2-5	4.25	11.50	0.0	0.037	1.20	1.0
LCG condition	Case 3-1	4.25	11.12	+2.0	0.037	1.20	1.0
	Case 3-2	4.25	11.12	+1.0	0.037	1.20	1.0
	Case 3-3	4.25	11.12	0.0	0.037	1.20	1.0
	Case 3-4	4.25	11.12	-1.0	0.037	1.20	1.0
	Case 3-5	4.25	11.12	-2.0	0.037	1.20	1.0
Friction coefficient	Case 4-1	4.25	11.12	0.0	0.025	1.20	1.0
	Case 4-2	4.25	11.12	0.0	0.030	1.20	1.0
	Case 4-3	4.25	11.12	0.0	0.035	1.20	1.0
	Case 4-4	4.25	11.12	0.0	0.037	1.20	1.0
	Case 4-5	4.25	11.12	0.0	0.040	1.20	1.0
	Case 4-6	4.25	11.12	0.0	0.045	1.20	1.0
	Case 4-7	4.25	11.12	0.0	0.050	1.20	1.0
	Case 4-8	4.25	11.12	0.0	0.055	1.20	1.0
	Case 4-9	4.25	11.12	0.0	0.060	1.20	1.0
Drag coefficient	Case 5-1	4.25	11.12	0.0	0.060	1.40	1.0
	Case 5-2	4.25	11.12	0.0	0.060	1.20	1.0

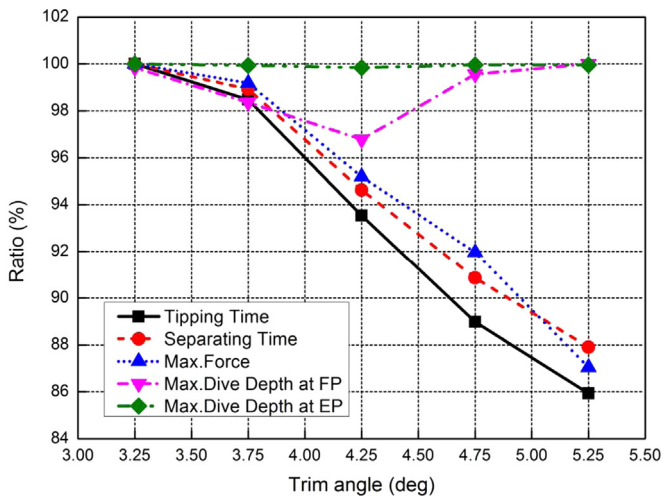


Fig. 19. Variations in launching responses versus the barge trims.

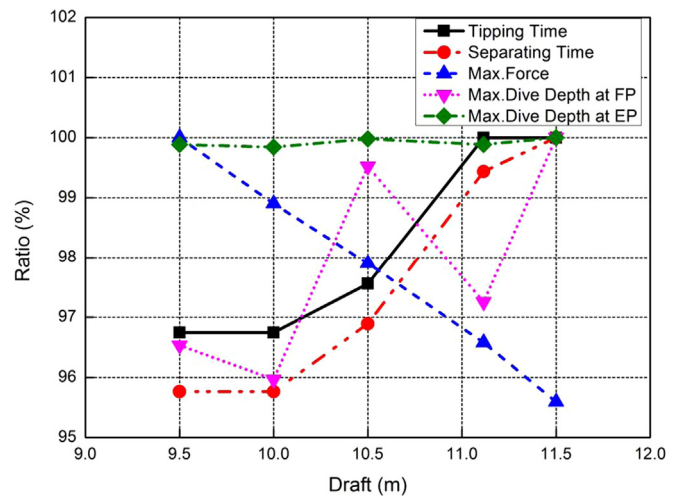


Fig. 20. Variations in launching responses versus the barge drafts.

stage, thereby increasing the hydrodynamic force on the jacket, directly reduces the maximum rocker load.

Fig. 20 shows the influences of the barge draft on the jacket motion and the maximum rocker load. A slight correlation is observed between the draft and the maximum rocker load. More specifically, compared with case 2-1, the maximum rocker loads in cases 2-2, 2-3, 2-4 and 2-5 are reduced by 1.10%, 2.10%, 3.42% and 4.41%, respectively. This indicates that a large draft can also reduce the maximum rocker load. The opposite relationship is observed between the tipping time and the draft. In addition, there is no explicit correlation between the maximum dive depth and draft. One possible reason for this phenomenon may be that the buoyancy increases due to the larger displacement, which results in a longer tipping time. Correspondingly, the maximum rocker load decreases slightly with a larger draft due to the compensation for the jacket weight by the buoyancy.

One of the interesting findings is that the trim angle has a greater effect than the draft in terms of the maximum rocker load. With cases 1-1 and 2-1 as references, the load ratios versus variations in the trim and draft are illustrated in Fig. 21. For a 3% increase in the maximum rocker load, the variations in the draft and trim angle are 1.31 m and 0.73°, respectively. This indicates that a smaller trim variation results in the same rocker load variation. A similar phenomenon was observed in the numerical simulations performed by Jo et al. (2002).

6.3.2. Longitudinal position of the jacket COG

Fig. 22 shows the influences of the jacket LCG on the motion responses and rocker loads. A positive LCG deviation means that it moves closer to the barge stern, whereas a negative value indicates a farther distance from the barge stern. As shown in Fig. 22, the maximum dive depth of the FP is reduced by 11.3% as the deviation

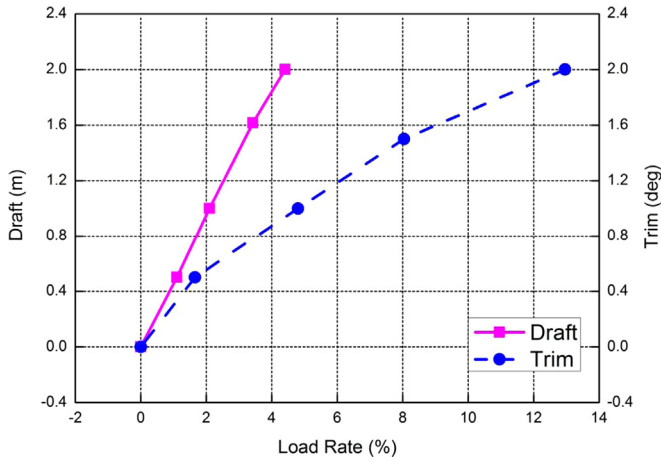


Fig. 21. Comparison of the effects of trim and draft on the maximum rocker load.

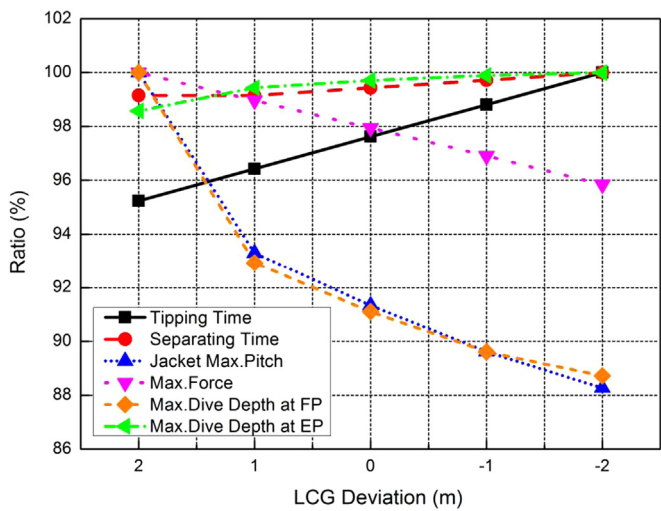


Fig. 22. Variations in launching responses versus the jacket LCG deviations.

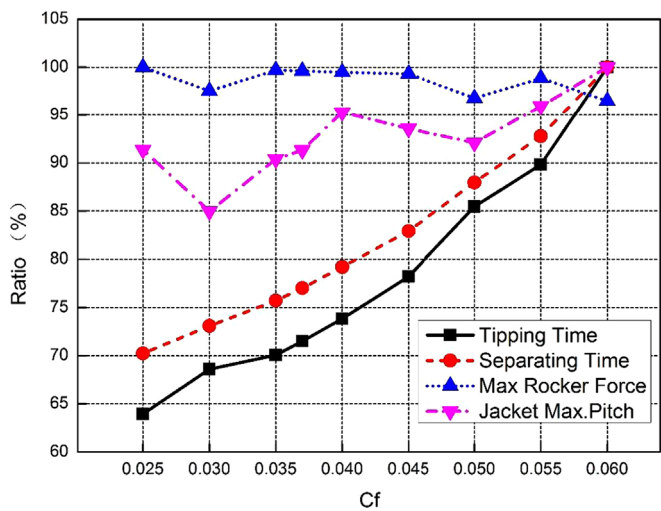


Fig. 23. Variations in launching responses versus friction coefficients.

of the jacket LCG changes from +2.0 m to -2.0 m, and the corresponding value of the EP increases by 1.44% with the same LCG variation. In addition, a longer duration will be generated when the jacket COG moves farther from the barge stern. According to these data, the jacket LCG is closely related to the jacket pitch

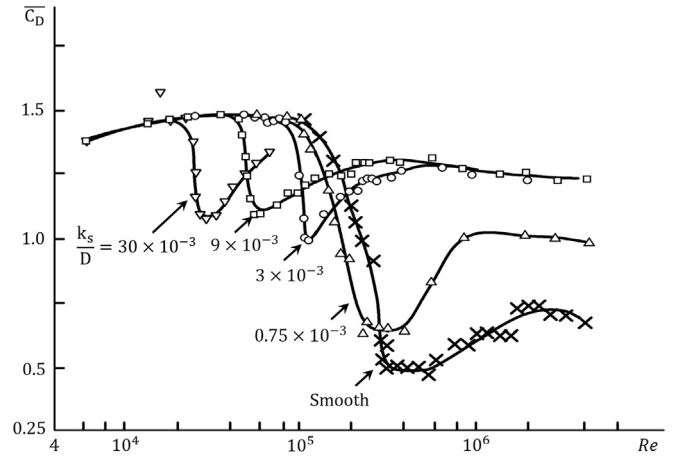


Fig. 24. Drag coefficient of a circular cylinder for various values of the surface roughness parameters k_s/D . (Achenbach and Heinecke, 1981).

motion. As the jacket COG moves farther from the barge stern, the jacket pitch angle increases (bow down) and, consequently, the maximum dive depth of the FP increases. Another interesting phenomenon observed in Fig. 22 is that the jacket pitch motion is clearly related to the maximum dive depth of the FP. Similar trends are observed in the variations of the maximum pitch angle and the maximum dive depth of the FP versus the LCG deviation. This trend indicates that the vertical motion of the FP can be greatly affected by the jacket pitch motion.

From the structural load perspective, the maximum rocker loads in cases 3-2, 3-3, 3-4 and 3-5 are reduced by 1.04%, 2.06%, 3.09% and 4.16%, respectively, versus the case 3-1. Moreover, the tipping time increases by 5.0% as the jacket LCG deviation varies from +2.0 m to -2.0 m. As discussed above, when the jacket COG passes over the tilting beam, the jacket starts to tip on the rocker arms. At the tipping time, the effect of the negative LCG deviation, thereby increasing the displacement of the jacket, is to increase the buoyancy and hydrodynamic forces and therefore reduce the rocker loads.

In general, the jacket LCG plays a very important role in a launching operation from the perspective of motion and structural load. It is desirable to move the jacket COG towards the barge bow to optimize the rocker loads and the subsequent upending operation.

6.3.3. Kinetic friction coefficient (C_f)

To investigate the influence of C_f along the skid-ways, the variations in the rocker load and motion response under certain C_f conditions are presented in Fig. 23. As shown in Fig. 23, the jacket motion responses are significantly affected by C_f , particularly the tipping time and separating time. As C_f increases from 0.025 to 0.060, the tipping time and separating time increase by 56.4% and 42.4%, respectively. Rodríguez et al. (2014) investigated the dynamic friction coefficient and its influences on the jack-up platform launching using an experimental approach. These authors reported that a smaller C_f could shorten the sliding duration of the jacket along the launch-ways. Additionally, no clear effect of C_f on the maximum rocker load and the maximum jacket pitch is observed. The friction coefficient must be sufficiently low to enable such gravity-driven launching.

6.4. Drag coefficient (C_D)

From the above results, there are differences in the launching behaviours between the experiment and field measurement. Several possible reasons for these differences in the Froude-

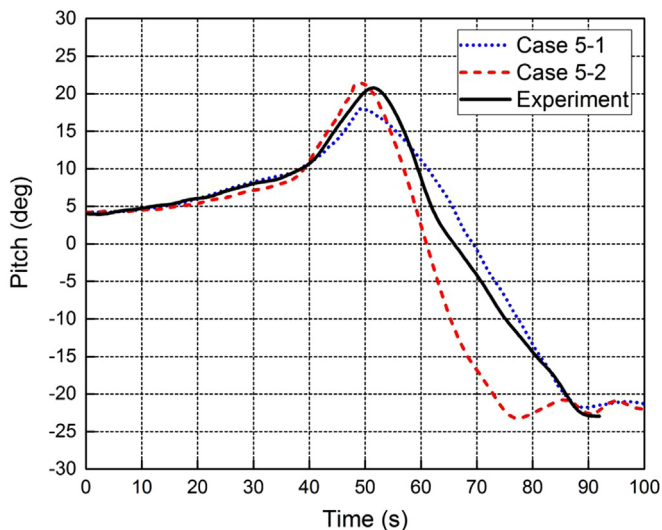


Fig. 25. Comparisons of pitch motions recorded in experiment, numerical case 5-1 and case 5-2.

Table 4

The launching responses recorded in the experiment, the numerical case 5-1 and case 5-2.

Items	Units	Experiments	Case 5-1	Case 5-2
Tipping time	s	36.9	36.4	34.7
Separating time	s	49.5	47.7	47.5
Max jacket pitch	deg	20.8	18.0	21.0
Max dive depth at FP	m	-97.3	-81.6	-99.3
Max dive depth at EP	m	-94.4	-92.7	-95.4
Max rocker load	MT	6333.0	6141.4	6365.1
Percent of jacket weight	%	27.2%	26.3%	27.3%

similarity models include C_f and C_D . As discussed before, the hydrodynamic force acting on the jacket is closely related to C_D . The estimated Re in the prototype is 2.5×10^6 , and that in the scaled model is approximately 8.5×10^3 . C_D is a function of the Re and roughness parameter (k_s/D), where k_s is the Nikuradse equivalent sand roughness (Sumer, 2006). Fig. 24 shows C_D plotted as a function of these parameters (Achenbach and Heinecke, 1981). As shown in Fig. 24, C_D ranges from 1.4 to approximately 1.0 in the case of employing a rough cylinder with $k_s/D = 3 \times 10^{-3}$. To investigate the effect of C_D , the numerical simulations in the full scale (Case 5-1 and 5-2) are performed and compared with the experiment.

Fig. 25 shows the time series of the pitch motions observed in the experiment, case 5-1 and case 5-2, respectively. As shown in Fig. 25, the launching operations in case 5-2 progress a little more rapid than that in case 5-2 and experiment. The tipping time in case 5-2 is approximately 34.7 s, while the jacket begins to tip at 36.4 s in case 5-1 and at 36.9 s in the experiment. And the maximum pitch angle in case 5-2 (21.0°) is slightly larger than that in the experiment (20.8°) and case 5-1 (18.0°). A possible explanation for the differences may be that the larger hydrodynamic forces on the scaled model can slow down the launching and marginally reduce the pitch motion in the case of employing the same friction coefficient (0.06).

To further understand the effect of C_D , the statistics of the launching responses in case 5-1, case 5-2 and experiment are summarized in Table 4. It can be seen from Table 4 that the maximum dive depth of the FP in case 5-2 is larger than that in the experiment and case 5-1, which shows a correlation between the maximum dive depth of the FP and the maximum pitch angle.

With regard to the maximum rocker loads, the comparisons show that C_D can have a modest influence.

As discussed before, the difference in C_f may induce a marked discrepancy in the launching duration between the model tests and field measurements. A larger C_f in the model test can introduce a significant time delay for the jacket launching operation. While the influence of C_D on the launching response could be quite modest. In general, gravity and friction are predominant during the sliding stage, and thus the effect of C_f is more reflected in the tipping time. While the buoyancy, friction and hydrodynamic forces are important during the tipping stage. The effect of C_D may be more reflected in the launching response during the tipping stage.

7. Conclusions

By comparing the jacket launching behaviours obtained from three different methods, the motion responses and the rocker arm loads are comprehensively investigated. This study yields the following conclusions:

1. Field measurements successfully captured dynamic launching processes when 6 DOFs motions and rocker loads are measured, which confirmed the safe operation of mega jacket launching. Moreover, field data provided more valuable information for future numerical simulations and model tests for jacket launching operations.
2. The model tests underestimate the maximum rocker load and over-predict the time needed to reach the tipping stage. Specifically, C_f along the skid-ways exhibits obvious influence on the time delay in the model test. Therefore, it is suggested that several sets of model tests with different C_f be carried out. Moreover, the differences in the environmental conditions and C_D could have a modest influence on the launching responses. It is also suggested that the launching tests be performed in a design sea state to predict the full-scale launching as comprehensively as possible. Although the model tests differ from the field launching in the launching duration, such tests could provide the quantification of the maximum rocker load and the maximum dive depth of the jacket.
3. As revealed by a sensitivity study, the jacket pitch motions and the maximum dive depths of the forward point and endpoint are sensitive to the LCG deviations of the jacket, which may pose a challenge in jacket design and fabrication. From the loads perspective, a larger barge trim and draft and a negative LCG deviation are favourable.

It should be recalled, however, that the measurement errors of the integrated GPS and INS system are not negligible, especially when the jacket reaches a great dive depth. The maximum dive depths obtained from the field measurement could be rather approximate. Further research is needed to improve the measurement methods and to bring better understanding to the jacket launching.

Acknowledgement

The authors would like to acknowledge the support of the National Natural Science Foundation of China (Grant nos. 51239007). Special thanks are given to Prof. Longfei Xiao and Mr. Lingzhi Xiong for their constant support and valuable suggestions.

References

- Achenbach, E., Heinecke, E., 1981. On vortex shedding from smooth and rough cylinders in the range of Reynolds numbers 6×10^3 to 5×10^6 . *J. Fluid Mech.* 109, 239–251.
- Chen, M.S., Taylor, R.E., Choo, Y.S., 2014a. Time domain modeling of a dynamic impact oscillator under wave excitations. *Ocean. Eng.* 76, 40–51.
- Chen, Y., Chen, G., Yang, J., Li, X., Jiang, X., 2014b. Research on field measurement of mega jacket launch. *Ocean. Eng.* 32 (6), 10–15.
- Chen, Y., Li, X., Chen, G., Li, G., Zhang, D., 2013. The use of INS and GPS and the post-processing method in field measurement of mega jacket launch. In: Proceedings of 32nd International Conference on Ocean Offshore and Arctic Engineering. Nantes, France, OMAE 2013-11482.
- Denton, G.N., 2013. Guidelines for the Transportation and Installation of Steel Jackets. GL Noble Denton.
- DNV, 2014. Environmental Conditions and Environmental Loads. Det Norske Veritas, Norway.
- Drazen, D., Eric, T., Don, W., Hazard, J., Cook, T., Scott, S., 2012. Full-scale measurements of wave impact loading on a flat plate. *ASME J. Offshore Mech. Arc. Eng.*, 449–458.
- Eagleson, H.V., 1945. An experimental method for determining coefficients of sliding friction. *Am. J. Phys.* 13 (1), 43–44.
- Fossen, T.I., 2011. Handbook of Marine Craft Hydrodynamics and Motion Control. John Wiley & Sons.
- Hambro, L., 1982. Jacket launching simulation by differentiation of constraints. *Appl. Ocean. Res.* 4 (3), 151–159.
- He, M., Li, H., Wang, A.M., Liang, Y., Li, X., Li, J., 2013. A comparative study of launch analysis and field measurement for liwan 3-1 mega jacket launch in south china sea. In: Proceedings of the 23rd International Offshore and Polar Engineering Conference. Anchorage Alaska, USA, pp. 822–831.
- He, M., Li, H., Wu, Z., Yu, W., Qian, J., Wang, A.M., 2010. Jacket launch and self-upending analyses with small-hole flooding scheme. In: Proceedings of the 20th International Offshore and Polar Engineering Conference. Beijing, China, pp. 400–407.
- Honarvar, M., Pirooz, M.D., Bahaari, M.R., 2008. A physical and numerical modeling for launching of jackets (Case Study on Balal PLQ Platform). *ASME J. Offshore Mech. Arc. Eng.* 130 (3), 031004.
- Jo, C.H., Kim, K.S., Lee, S., 2002. Criterion of offshore jacket launching analysis. In: Proceedings of the 11th International Offshore and Polar Engineering Conference. Stavanger, Norway, pp. 90–96.
- Jo, C.H., Kim, K.S., Lee, S., 2002. Parametric study on offshore jacket launching. *Ocean. Eng.* 29 (15), 1959–1979.
- Liu, Y., Yabin, G., Shuhua, G., 1986. Theoretical calculation and model test of jacket launching process. *Shipbuild. China* 1, 000.
- Micron Optics, 2012. User Guide, Revision 1.138. Micron Optics, Inc. 1852 Century Place NE, Atlanta, Ga. 30345 USA.
- Nachlinger, R., 2006. How MOSES Deals with Technical Issues. Ultramarine Inc.
- Rodríguez, C.A., Moura, M., Esperança, P.T.T., Raigorodsky, J., 2014. An experimental approach for the offshore launching of jack-ups. *ASME J Offshore Mech. Arc. Eng.* 136 (2), 021301.
- Sircar, S., Chandra, T., Mills, T., Roberson, W., 1990. Transportation launch and self-upend analysis of the kilauea jacket using proven analytical techniques. In: Proceedings of Offshore Technology Conference (OTC) 1990, Houston, Texas.
- Sumer, B.M., 2006. Hydrodynamics Around Cylindrical Structures. World Scientific.
- Tyler, S., Silvia, T., Claire, D., 2013. Strain measurements using fibre Bragg gratings during full-scale structural testing of an F/A-18 centre barrel. *Key Eng. Mater.* 558, 510–521.
- Xiong, L., Yang, J., Li, X., Xu, X., 2013. Study on numerical simulation of jacket launching progress. In: Proceedings of 32nd International Conference on Ocean, Offshore and Arctic Engineering. Nantes, France, OMAE 2013-11178.
- Xu, X., Yang, J., Li, X., Lu, H., 2013. Investigation on hydrodynamic performance of T-shaped barge in topside transportation. *J. Ship Mech.* 17 (12), 1426–1438.
- Zhang, D., Li, X., Li, D., Liang, Y., Yang, Z., Sun, X., Wang, A.M., 2013. A model test study for liwan 3-1 mega jacket launch in South China Sea. In: Proceedings of the 23rd International Offshore and Polar Engineering Conference. Anchorage, Alaska, USA, pp. 814–821.
- Zhao, W., Yang, J., Hu, Z., Tao, L., 2014. Coupling between roll motions of an FLNG vessel and internal sloshing. *ASME J Offshore Mech. Arc. Eng.* 136 (2), 021102.



این مقاله، از سری مقالات ترجمه شده رایگان سایت ترجمه فا میباشد که با فرمت PDF در اختیار شما عزیزان قرار گرفته است. در صورت تمایل میتوانید با کلیک بر روی دکمه های زیر از سایر مقالات نیز استفاده نمایید:

لیست مقالات ترجمه شده ✓

لیست مقالات ترجمه شده رایگان ✓

لیست جدیدترین مقالات انگلیسی ISI ✓

سایت ترجمه فا ؛ مرجع جدیدترین مقالات ترجمه شده از نشریات معتبر خارجی